

# Oxygen-barrier films based on low-density polyethylene/ethylene vinyl alcohol/ polyethylene-grafted maleic anhydride compatibilizer

Mohammadreza Rahnama, Abdulrasoul Oromiehie, Shervin Ahmadi\*, Ismaeil Ghasemi

Department of Plastics Engineering, Iran Polymer and Petrochemical Institute, P.O.Box14975/112, Tehran, I.R. Iran

Received: 29 August 2016, Accepted: 2 October 2016

## ABSTRACT

In this research, high oxygen-barrier films were organized based on low-density polyethylene (LDPE)/ ethylene vinyl alcohol (EVOH)/ polyethylene-grafted maleic anhydride (LDPE-g-MA) compatibilizer. The effects of 10–30 wt. % EVOH and 0–10 wt. % LDPE-g-MA loadings on the properties of final films were evaluated. The morphology of specimens was observed by using scanning electron microscopy (SEM). Oxygen transfer rate (OTR) results revealed that the addition of EVOH up to 30 wt. % to neat LDPE could significantly decrease oxygen permeability. The LDPE-g-MA which increased the permeability needed to be fine-tuned its amount based on the EVOH loading in different samples. The experimental results revealed that the addition of 30 wt. % EVOH to the LDPE matrix without adding LDPE-g-MA gave the best oxygen barrier properties. Elastic modulus and tensile strength increased with incorporation of EVOH and LDPE-g-MA into the polyethylene matrix. On the other hand, elongation-at-break decreased with the addition of EVOH and increased with the introduction of compatibilizer to the samples. Incorporation of EVOH and LDPE-g-MA into the LDPE matrix and increasing their amounts led to higher storage modulus and zero shear rate viscosity, but lowered the frequency value at the intersection point of storage modulus ( $G'$ ) and loss modulus ( $G''$ ). The only exception was that in the samples without compatibilizer, the increase in the EVOH content resulted in a lower zero shear rate viscosity and a higher frequency value at the intersection point of  $G'$  and  $G''$ . **Polyolefins J (2017) 4: 137-147**

**Keywords:** Polymer blends and alloys; barrier; compatibilizer; oxygen permeability; polyethylene.

## INTRODUCTION

Nowadays, packaging is one of the most interesting research fields in the food industries [1, 2]. Plastic material with high gas and solvent barrier properties is found to be highly advantageous compared to metal and glass alternatives for use in applications such as packaging and gasoline tanks [3, 4]. The main properties required for a suitable packing are oxygen permeability, clar-

ity, suitable mechanical properties, processability, recyclability and low cost of production [5, 6]. One of the most important requirements is low permeability to gases and hydrocarbons [7-9]. Beside the permeability, the mechanical properties should also meet product specifications. Generally, one polymeric material cannot alone offer all the properties required, therefore, a combination of polymers is required. For this purpose, the multi-layer packaging is suggested [5, 6]. This kind

\* Corresponding Author - E-mail: Sh.Ahmadi@ippi.ac.ir

of packaging, however, requires quite expensive multi devices and processing. In addition, recycling of final product is difficult as well as the clarity of product could not be retained [10, 11]. Then, in order to eliminate such troubles, compounding is suggested as a possible alternative. Compounding is a cost-effective method which utilizes different properties of two or more polymers, simultaneously [12-14].

Polyethylene owing to its excellent properties such as easy processing, high toughness in low temperatures, reasonable price, good electrical resistance, and excellent humidity barrier, is one of the best choices for food packaging. High permeability to gases such as O<sub>2</sub> and CO<sub>2</sub> is one of the most important weaknesses of polyethylene usage in packaging [15, 16].

On the other hand, ethylene vinyl alcohol random copolymer as a semi-crystalline polymer with excellent resistance against solvents, aromatics, and gases [11, 17] has so many applications [18-20]. Low permeation in this polymer is a result of strong intermolecular hydrogen-bonding interactions [11, 21]. Its high moisture absorption and low resistance against permeation of moisture are undesirable in food packaging industry and attenuate its barrier properties against oxygen penetration [22]. Water molecules act as a softener and weaken hydrogen bonding, resulting in a reduction in the barrier properties [3]. Beside of the mentioned problem, EVOH is brittle in nature and quite expensive, so blending of this polymer with polyethylene is the best choice to overcome the mentioned polymer's problems [23, 24].

Most commercial EVOH materials contain 55 to 75 mole percent vinyl alcohol, which is a polar component with effective gas barrier performance. This component is not compatible with polyethylene (a nonpolar polymer) [25]. Incompatibility between these two polymers leads to formation of the morphologically unstable and brittle blends. For compatibilizing two immiscible polymers in a blend, using a compatibilizer is a common practice [11, 25]. However, it should be noted that the use of a proper amount of compatibilizer and applying a suitable process for polymer blending are critical factors affecting on the properties of final products [26, 27]. For example, the presence of an extra quantity of compatibilizer could lead to a complete distribution of oxygen-barrier polymer

and loss of vital oxygen permeability resistance in a EVOH/polyethylene blend. Therefore, the amount of the compatibilizer has to be fine-tuned to achieve planar morphology of dispersing phase of EVOH in polyethylene as the continuous phase [28].

Different kinds of compatibilizers such as ionomer [29], high-density polyethylene (HDPE)-g-MA [30] [30-33], and hydrogenated and maleic anhydride-grafted SEBS (SEBS-g-MA) [31] have been used by researchers for the preparation of polyolefin/ EVOH blends. Functionalization of the polymeric phases is another method [31, 34] applied to increase the compatibility of these phases. The results of these studies showed that the use of compatibilizer or functionalization improved the compatibility of two phases and led to achieve better barrier and mechanical properties.

In this study, packaging films with high oxygen barrier properties were prepared based on LDPE/ EVOH/ LDPE-g-MA blends. The main objective of this work was to evaluate the effect of changing composition of different phases on the properties of the final product. The content of each phase including EVOH (10-30 wt%) and the compatibilizer (0-10 wt%) was changed in three levels in the LDPE matrix. Mechanical, permeability and morphological properties were investigated. Since the melt rheology affected the final morphology of the blends, the rheological properties were studied profoundly.

## EXPERIMENTAL

### Materials

EVOH grade DC3203RB (32 mol % ethylene content) was purchased from Soarnol, UK with a melt flow index (MFI) of 3.8 g/10 min (2.16 kg, 210°C) and density of 1.19 g/cm<sup>3</sup>. The LDPE 0020 with an MFI of 2 g/10 min (2.16 kg, 190°C) and density of 0.920 g/cm<sup>3</sup> was purchased from Bandar Imam Petrochemical Complex, Iran. LDPE-g-MA (1.5 wt% maleic anhydride grafted) with an MFI of 1.2 g/10 min (2.16 kg, 190°C) and density of 0.923 g/cm<sup>3</sup> was obtained from Karangin Co., Iran.

### Sample preparation

Samples were prepared by melt blending process us-

ing a twin-screw extruder (Brabender, Germany, L/D=40) with a temperature range of 180–220°C at 100 rpm. The extruder heating zones were set for 180, 190, 200, 210, 215 and 220°C. Initially, an LDPE/LDPE-g-MA blend having 20 wt% of LDPE-g-MA was compounded. Then, concerning the composition of each sample, final samples were provided via melt blending. The composition of different samples is shown in Table 1.

Finally, film blowing technique by using a single screw extrusion system (Brabender, Germany, L/D=26) operated at the temperature range of 180–220°C and 100 rpm using a 20 mm die diameter was employed for production of each sample film specimen. The final films prepared by the blowing process were 20 cm in width and about 100±5 µm in thickness.

### Characterization

The morphological study of each specimen was done with a VEGA model SEM apparatus (Tescan, Czech Republic). Dimethyl sulfoxide was used as a solvent for extraction of EVOH from blends. The samples were etched for 4 to 6 h at 50°C and dried for 24 h at 50°C. The samples were then freeze-fractured in liquid nitrogen, gold-sputtered, and their cross-section was used for SEM studies. Using a GDP-C gas permeability tester (Coesfeld Meteriatest, Germany), the films' OTR was tested according to ASTM D3985. The diameter of round samples prepared for oxygen permeability test was 150 mm and the average thickness of each sample was 100±5 µm. The test was performed in triplicate and at a temperature of 23°C and relative humidity of 50%. An SFM 500 tensile machine (Santam, Iran) was used to study the mechanical properties. The dimensions of the specimens for the tensile test were 10×60 mm according to ASTM D882. The

rheology tests were performed at T=200°C under a nitrogen atmosphere. Dynamic melt rheological experiments were conducted in a modular compact rheometer (MCR 300) from Physica in parallel plates (25 mm diameter, 1 mm gap) mode. At first, strain sweep test was carried out to find the linear region of the samples at 200°C on sample 9. This sample was selected because it had the maximum amount of EVOH and LDPE-g-MA among the samples and displayed the maximum nonlinearity. The sample revealed a linear behavior until 15% strain. Dynamic melt rheological properties including complex dynamic viscosity,  $G'$ , and  $G''$  were measured with a frequency sweep test between 0.02 to 600 rad/s at 5% strain to ensure being in the linear viscoelastic region.

## RESULTS AND DISCUSSION

### Morphological study

Morphology of the blends was studied by SEM test. The SEM micrographs of the specimens numbered 2, 4, 6, and 8 are shown in Figure 1.

Samples 4 and 6 were chosen since they had the same amount of EVOH (20 wt%) but different amounts of the compatibilizer. Also, samples 2 and 8 had the same amount of LDPE-g-MA (5 wt%) but different amounts of the EVOH. So, the effect of the presence and the level of compatibilizer and EVOH on the dispersion of EVOH phase in the matrix could be evaluated easily.

SEM images (b and c) in Figure 1 indicate that the presence of excessive compatibilizer leads to the unnecessary dispersion of EVOH in the LDPE matrix. The aforesaid effect could cause the elimination of EVOH desirable planar morphology which in turn degenerated the blend's barrier properties. It can be seen there is the semi-planar morphology in the sample without compatibilizer (sample 4). The other SEM Images (a and d) in Figure 1 show that increment of EVOH level from 10 to 30 wt% in the samples with the same amount of compatibilizer (5 wt%) leads to changing the droplet-like morphology of EVOH in the LDPE matrix to the planar morphology. The aforementioned result shows that the amount of compatibilizer must be fine-tuned based on the EVOH level in

**Table 1.** Composition of different samples.

Samples	EVOH (wt%)	LDPE-g-MA (wt%)	LDPE (wt%)
1	10	0	90
2	10	5	85
3	10	10	80
4	20	0	80
5	20	5	75
6	20	10	70
7	30	0	70
8	30	5	70
9	30	10	60

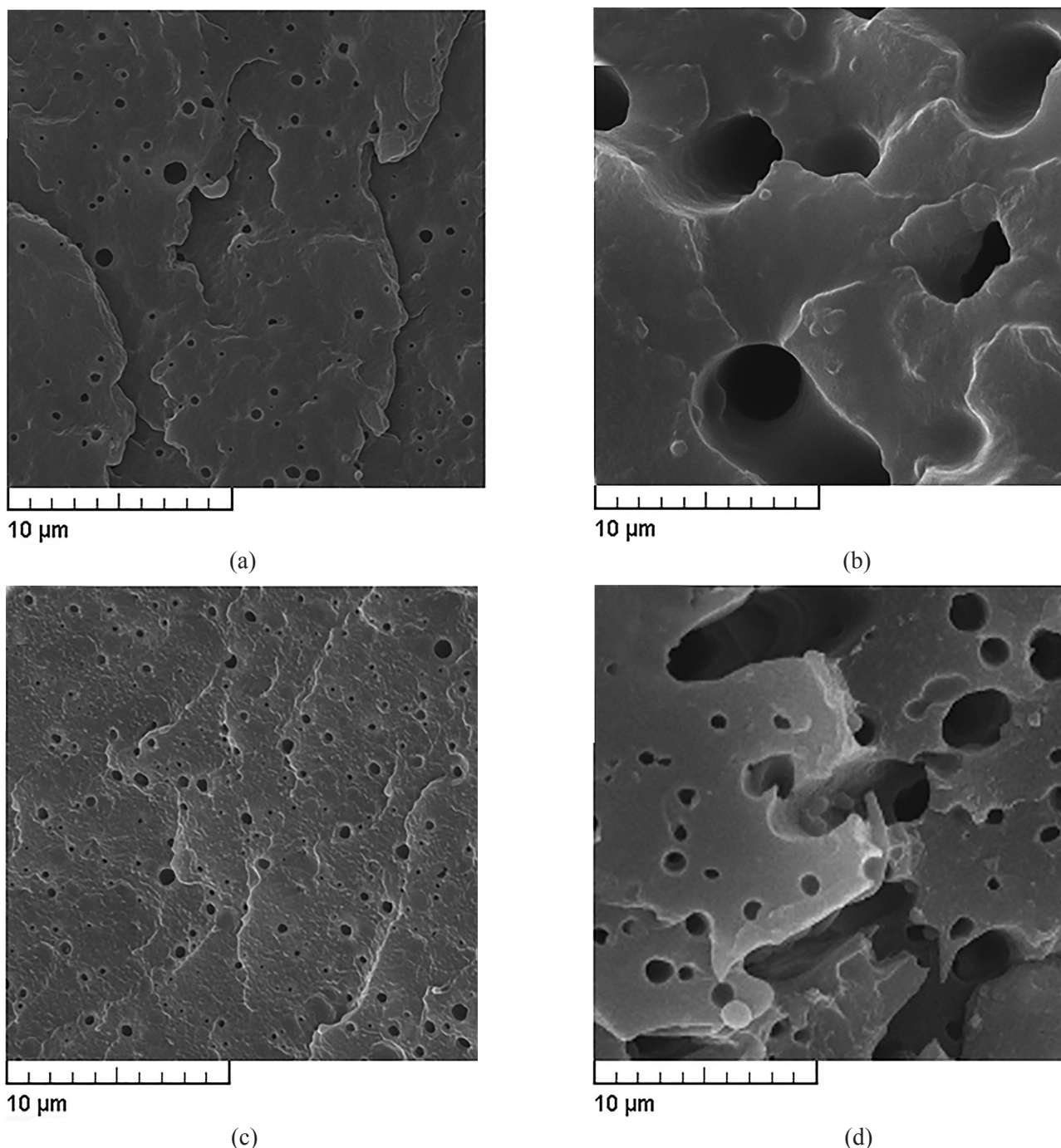


**Figure 1.** SEM micrographs of a) sample 2, b) sample 4, c) sample 6, and d) sample 8.

different samples. For example, the use of 5 wt% compatibilizer is adequate for the samples containing 30 wt% EVOH while the same weight percent will be surplus for the samples containing only 10 wt% of EVOH.

#### Oxygen transfer rate

OTR results for different samples are demonstrated in Table 2.

Figure 2 shows the OTR results for different samples.

It is obvious in Figure 2 that by increasing the EVOH level, oxygen permeation has reduced from 1400 cc/m<sup>2</sup>.day.atm for neat LDPE to less than 100 cc/m<sup>2</sup>.day.atm for the samples with 30 wt% EVOH. The superior barrier property of EVOH against oxygen penetration is the reason of this incident. According to tortuous path theory, the presence of EVOH layers results in

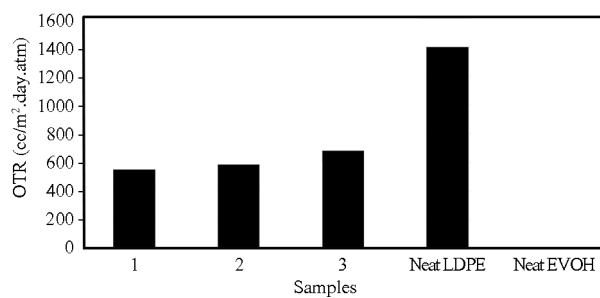
**Table 2.** OTR results for different samples.

Samples	OTR (cc/m <sup>2</sup> .day.atm)
1	550.00
2	585.00
3	678.80
4	249.00
5	285.40
6	363.00
7	23.00
8	51.00
9	84.20
Neat LDPE	1400.00
Neat EVOH	0.06

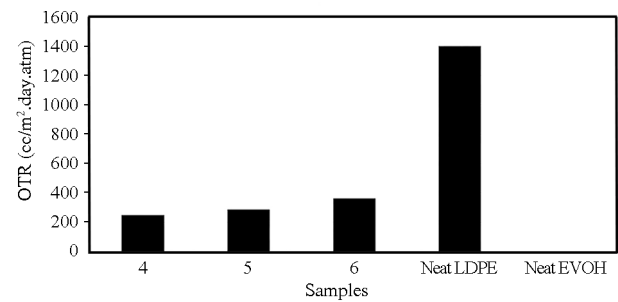
increased resistance of the final product to oxygen permeation [35, 36].

The compatibilizer can also slightly affect the penetration resistance. Based on Figures 1 and 2, an exces-

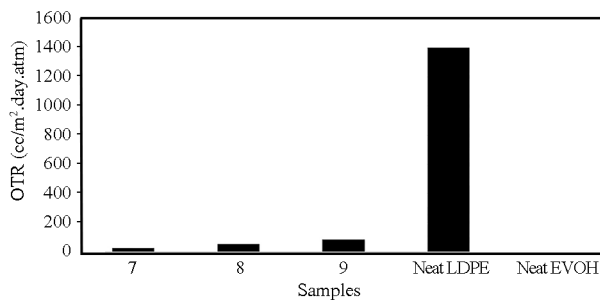
sive amount of compatibilizer results in a droplet-like morphology of EVOH, in the LDPE matrix which is undesirable, since the lamellar morphology is the best for improving barrier properties. According to Figure 2, the addition of 10 wt% LDPE-g-MA causes a decline in the barrier properties to even lower than those for the specimen without compatibilizer at all weight percents of EVOH. Among different samples, sample 7 has the minimum oxygen penetration. So, maximum amount of EVOH and compatibilizer absence lead to the highest barrier properties for the samples. Although, the compatibilizer presence leads to deterioration of barrier properties, the effect of its presence on the mechanical properties must be considered. In the following the mechanical properties are investigated



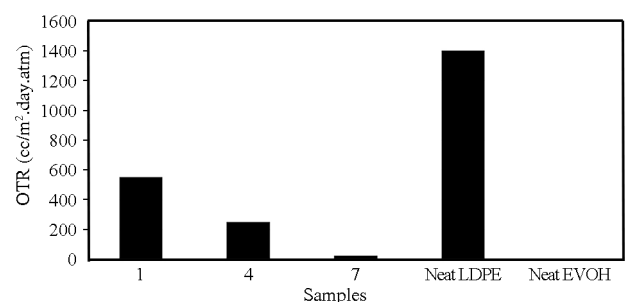
(a)



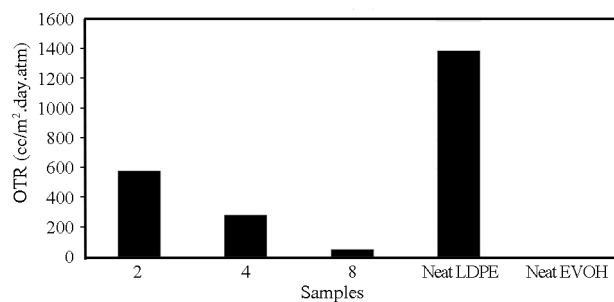
(b)



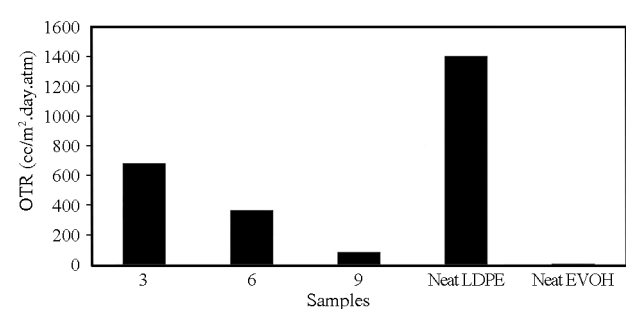
(c)



(d)



(e)



(f)

**Figure 2.** OTR results for a) samples containing 10 wt% EVOH, b) samples containing 20 wt% EVOH, c) samples containing 30 wt% EVOH, d) samples containing 0 wt% LDPE-g-MA, e) samples containing 5 wt% LDPE-g-MA, and f) samples containing 10 wt% LDPE-g-MA.

because of their importance on the film formation process.

### Mechanical properties

Table 3 demonstrates the mechanical properties (elongation-at-break, tensile strength and tensile modulus) for different samples.

Among tensile properties, elongation-at-break can be a good measure of compatibility evaluation. If the elongation-at-break value increases, preparation of the film becomes easier, therefore, higher elongation-at-break is preferable.

As predicted, the addition of EVOH declined the elongation-at-break (Table 3). EVOH is brittle in nature, and its introduction to the nanocomposite increases the elastic modulus while lowering the elongation-at-break as expected.

The addition of LDPE-g-MA to the blends can strengthen the interface bonding of EVOH and LDPE phases, leading to compatibilization of the phases and enhancing elongation-at-break. According to the achieved results, the higher elongation-at-break was found for the sample containing 10 wt% EVOH and 10 wt% LDPE-g-MA.

According to Table 3, the elastic modulus increases expectedly with the rise of EVOH level of the samples. When EVOH which is a brittle polymer with high elastic modulus is added to the LDPE matrix, the elastic properties of the final product, specially its elastic modulus, are enhanced based on the mixture law [37].

The presence of the compatibilizer also increases elastic modulus of the samples. Compatibilizer can

enhance the interfacial tension of the blends which leads to the improved compatibility of the phases. This phenomenon increases elastic modulus by reducing the count of weak points and enhances mechanical properties and elastic modulus of the blends.

The obvious improvement of tensile strength with increasing EVOH content in the samples could be attributed to the high tensile strength of EVOH and explained based on the mixture law [37]. Furthermore, tensile strength highly is influenced by the interface of EVOH and LDPE phases. The introduction of LDPE-g-MA into the samples leads to formation of a stronger boundary because of more compatibility between two phases. This augmentation results in the enhanced tensile strength of specimens.

### Rheological behavior

Figure 3 shows the storage modulus versus frequency for samples 2, 4, 6, 8, and neat LDPE.

Based on Figure 3, the addition of EVOH and the compatibilizer to the LDPE matrix has increased its storage modulus in comparison to that of neat LDPE. Since EVOH has a higher melting temperature and modulus compared to polyethylene, it can act as a solid object within the polyethylene matrix and rise the sample storage modulus. The addition of compatibilizer has the same effect due to improved dispersion of EVOH in the polyethylene matrix and strengthening the interface of EVOH and LDPE phases. The achieved results showed that the addition of 10 wt% EVOH and 5 wt% of the compatibilizer results in an almost equal growth in the storage modulus.

The graph of complex dynamic viscosity changes versus frequency for samples 2, 4, 6, 8, and neat LDPE are depicted in Figure 4.

The Carreau-Yasuda model was applied for more accurate study of changes in complex dynamic viscosity versus frequency in the low frequencies region of the graph, as follows:

$$\eta = \eta_0 [1 + (\tau\omega)^\alpha]^{-\frac{n-1}{\alpha}} \quad (1) [38]$$

Where  $\eta_0$  is the zero shear rate viscosity (the zero shear rate viscosity is the limit of the apparent viscosity of a melt when the shear rate approaches zero),  $\eta$  is the

**Table 3.** Mechanical properties of different samples.

Samples	Elongation-at-break (%)	Tensile strength (MPa)	Tensile modulus (MPa)
1	145.40	8.40	291.70
2	170.00	8.77	312.30
3	228.20	8.85	332.60
4	87.00	9.36	465.40
5	88.00	9.86	469.00
6	105.00	10.18	472.00
7	63.60	10.46	501.90
8	70.00	11.13	522.20
9	76.80	11.73	540.20
Neat LDPE	451.00	8.00	234.50
Neat EVOH	9.60	35.00	2546.00

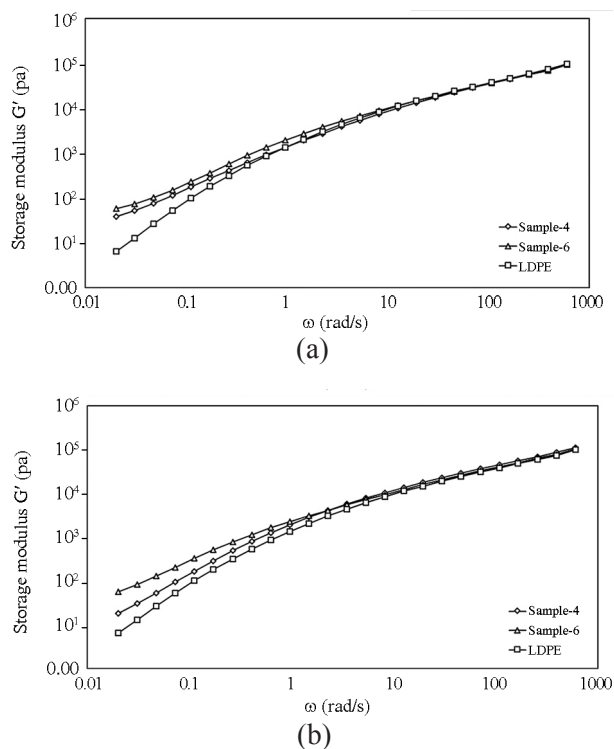


**Figure 3.** Storage modulus versus frequency for a) samples 4, 6, and neat LDPE and b) samples 2, 8, and neat LDPE.

relaxation time,  $n$  is the power-law index, and  $a$  is the width of the transition range between zero shear rate viscosity and power-law region. Table 4 displays these fitting parameters for different samples.

Based on Table 4, the addition of EVOH and the compatibilizer to the LDPE matrix as well as raising the level of these substances in the specimens increases the zero shear rate viscosity. For the samples without the compatibilizer, the addition of EVOH leads to the zero shear rate viscosity reduction.

This increase in the viscosity at low frequencies could be attributed to the strong interaction between the compatibilizer functional groups and EVOH that increase the interfacial tension toward the formation of thermodynamically stabilized morphology [30]. However, in the samples without compatibilizer, this interaction will be diminished and leads to the zero shear rate viscosity reduction.

The relaxation time  $\tau$  shows the same style as the zero shear rate viscosity. An increase of relaxation time can be interpreted as an increase in the elasticity of the samples. In the discussion about the intersection point of  $G'$  and  $G''$ , this matter will be further investigated.

The intersection of storage and loss moduli graphs

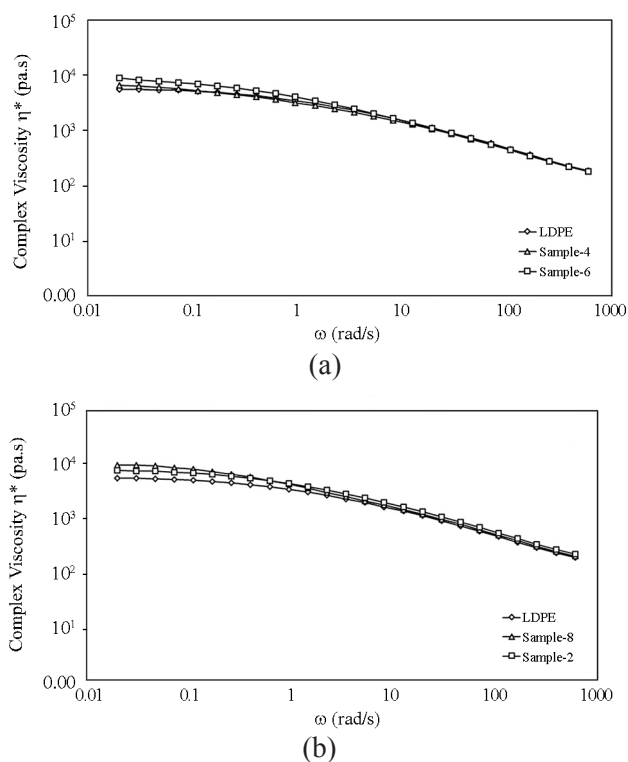


**Figure 4.** Complex dynamic viscosity versus frequency for a) samples 4, 6, and neat LDPE and b) samples 2, 8, and neat LDPE.

was studied to examine the elastic properties of the samples. It is well known that for creation of a final film, the elasticity and elastic properties of material are critical. Therefore, to further investigate the elastic properties of the samples, the intersection point of storage and loss moduli graphs was considered.

Figure 5 illustrates the frequency values at the intersection point of loss and storage moduli for various samples.

This point is recognized as the crossover modulus in which storage and loss moduli are equal. Where the storage modulus is greater than the loss modulus, polymer melt behavior is like a viscoelastic solid, however, with the increase of the loss modulus to greater values than that of storage modulus, polymer behavior becomes similar to a viscoelastic melt.

According to Figure 5, the addition of compatibilizer and EVOH as well as increasing their contents shifts the intersection point of loss and storage moduli to lower frequencies, which indicates an increase in the elastic behavior and relaxation time for the prepared nanocomposites. For the samples without the compatibilizer, the addition of EVOH leads to higher

**Table 4.** Carreau-Yasuda parameters for different samples.

Samples	$\eta_0$ (kPa.s)	$\tau$ (s)	$n$	$R^2$
2	8.60	1.16	0.44	0.99
4	8.57	0.79	0.39	0.99
6	10.29	2.12	0.43	0.99
8	12.29	3.73	0.47	0.99
Neat LDPE	6.03	0.84	0.44	0.99
Neat EVOH	4.28	0.05	0.43	0.99

intersection points. This phenomenon had also been seen in the modeling with using the Carreau-Yasuda model.

It has been reported that during film blowing process, the higher elasticity of polymer melt favors crystal orientation in the final samples. The films with oriented structures exhibit higher mechanical properties

and lower oxygen permeability [39-41].

## CONCLUSION

In this research, high oxygen-barrier films were organized based on LDPE/ EVOH/LDPE-g-MA, in which LDPE-g-MA acted as a compatibilizer. The effects of EVOH (10–30 wt%) and LDPE-g-MA (0–10 wt%) loadings on the properties of final films were evaluated. The results concluded from this study are listed as follows:

- OTR results revealed that the addition of EVOH up to 30 wt% to neat LDPE could significantly de-

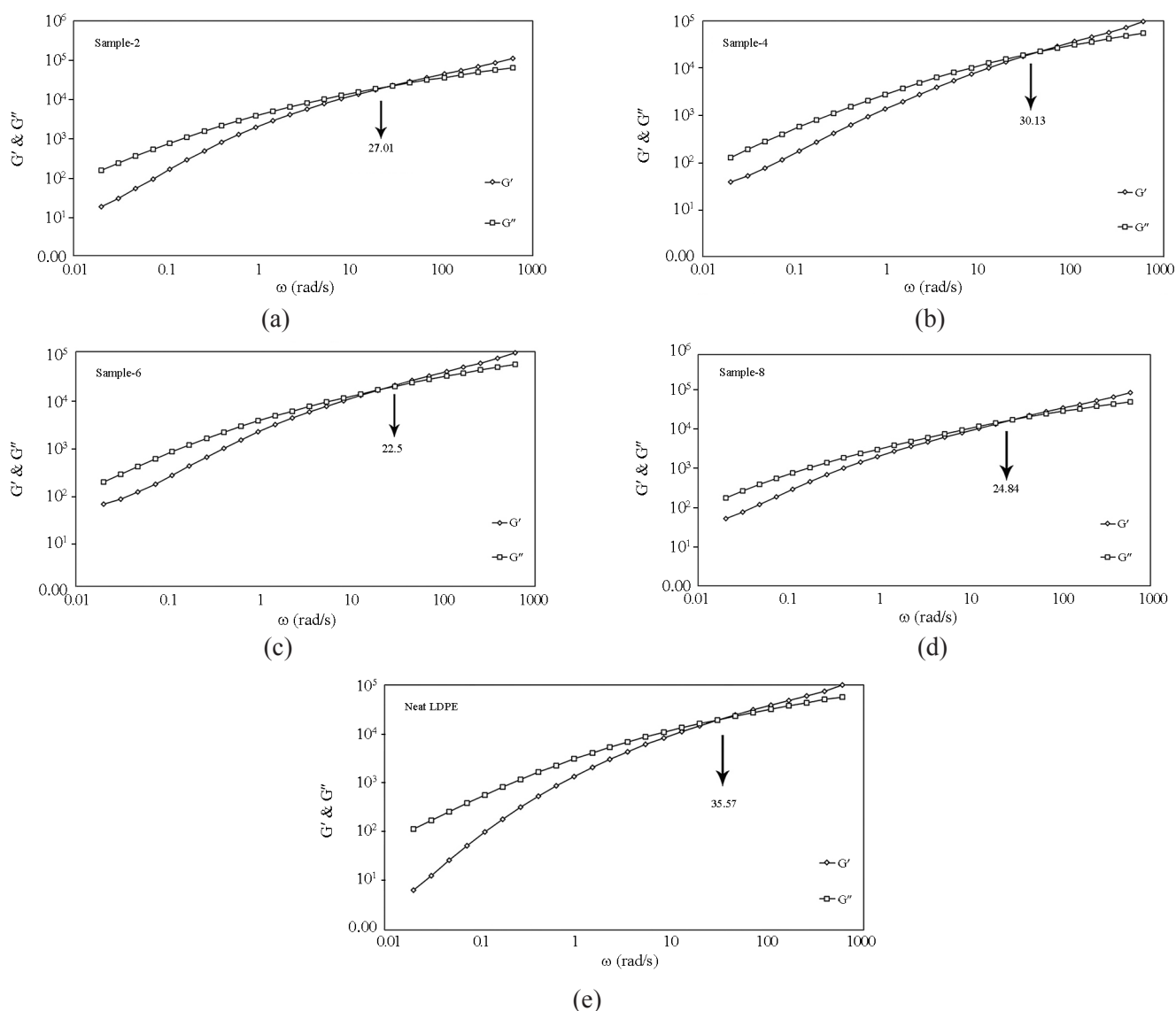


**Figure 5.** Frequency value at the intersection point of loss and storage moduli for a) sample 2, b) sample 4, c) sample 6, d) sample 8, and e) neat LDPE.



crease oxygen permeability. LDPE-g-MA which increased the permeability needed to be fine-tuned based on the EVOH level in different samples.

- Elastic modulus and tensile strength increased with the introduction of EVOH and LDPE-g-MA to the polyethylene matrix. On the other hand, elongation-at-break decreased with the addition of EVOH and increased with the introduction of compatibilizer to the samples.
- Incorporation of EVOH and LDPE-g-MA into the LDPE matrix and increasing the amount of these components in the samples led to higher storage modulus and zero shear rate viscosity, but, lowered the frequency at the intersection point of  $G'$  and  $G''$ . The only exception was that in the samples without compatibilizer, the increase of the EVOH loading resulted in a lower zero shear rate viscosity and a higher frequency value at the intersection point of  $G'$  and  $G''$ .

## REFERENCES

1. Duncan TV (2011) Applications of nanotechnology in food packaging and food safety: Barrier materials, antimicrobials and sensors. *J Colloid Interface Sci* 363: 1-24
2. Silvestre C, Duraccio D, Cimmino S (2011) Food packaging based on polymer nanomaterials. *Prog Polym Sci* 36: 1766-1782
3. Huang C-H, Wu J-S, Huang C-C, Lin L-S (2004) Morphological, thermal, barrier and mechanical properties of LDPE/EVOH blends in extruded blown films. *J Polym Res* 11: 75-83
4. Santamaría P, González I, Eguiazábal JI (2015) Mechanical and barrier properties of ternary nanocomposite films based on polycarbonate/amorphous polyamide blends modified with a nanoclay. *Polym Adv Technol* 26: 665-673
5. Robertson GL (2012) Food packaging: principles and practice. CRC press
6. Mathlouthi M (2013) Food packaging and preservation. Springer Science & Business Media
7. Lange J, Wyser Y (2003) Recent innovations in barrier technologies for plastic packaging-A review. *Packag Technol Sci* 16: 149-158
8. Elen K, Murariu M, Peeters R, Dubois P, Mullens J, Hardy A, Van Bael M (2012) Towards high-performance biopackaging: Barrier and mechanical properties of dual-action polycaprolactone/zinc oxide nanocomposites. *Polym Adv Technol* 23: 1422-1428
9. Scherzer T, Schubert R (1998) Oxygen permeability of electron beam cured gelatin methacrylate layers. *Polym Adv Technol* 9: 777-785
10. Ait-Kadi A, Bousmina M, Yousefi A, Mighri F (2007) High performance structured polymer barrier films obtained from compatibilized polypropylene/ethylene vinyl alcohol blends. *Polym Eng Sci* 47: 1114-1121
11. Rahnama M, Oromiehie A, Ahmadi S, Ghasemi I (2016) Investigation of polyethylene-grafted-maleic anhydride presence as a compatibilizer on various properties of nanocomposite films based on polyethylene/ethylene vinyl alcohol/nanoclay. *Polym Adv Technol*
12. Paul DR (2012) Polymer blends. Vol. 1., Elsevier
13. Mittal V (2012) Functional polymer blends: Synthesis, properties and performance, CRC Press
14. Gomari S, Ghasemi I, Karrabi M, Azizi H (2015) An investigation on non-isothermal crystallization behavior and morphology of polyamide 6/poly (ethylene-co-1-butene)-graft-maleic anhydride/organoclay nanocomposites. *Polyolefins J* 2: 99-108
15. Kebritchi A, Nekoomanesh M, Mohammadi F, Khonakdar HA (2014) The role of 1-hexene comonomer content in thermal behavior of medium density polyethylene (MDPE) synthesized using Phillips catalyst. *Polyolefins J* 1: 117-129
16. Zohuri G, Damavandi S, Ahmadjo S, Shamekhi M (2014) Synthesis of high molecular weight polyethylene using FI catalyst. *Polyolefins J* 1: 25-32
17. Mokwena KK, Tang J (2012) Ethylene vinyl alcohol: a review of barrier properties for packaging shelf stable foods. *Crit Rev Food Sci Nutr* 52: 640-650
18. Wang G, Yoshikawa H, Tamiya E, Uyama H (2015) Mesoporous poly (ethylene-co-vinyl alcohol) monolith captured with silver nanoparticles as a SERS substrate: Facile fabrication and ultra-

- high sensitivity. *RSC Adv* 5: 25777-25780
19. Wang G, Kundu D, Uyama H (2015) One-pot fabrication of palladium nanoparticles captured in mesoporous polymeric monoliths and their catalytic application in C–C coupling reactions. *J Colloid Interface Sci* 451: 184-188
  20. Wang G, Xin Y, Uyama H (2015) Facile fabrication of mesoporous poly (ethylene-co-vinyl alcohol)/chitosan blend monoliths. *Carbohydr Polym* 132: 345-350
  21. Kim SW, Cha SH (2014) Thermal, mechanical, and gas barrier properties of ethylene–vinyl alcohol copolymer-based nanocomposites for food packaging films: Effects of nanoclay loading. *J Appl Polym Sci* 131: 40289
  22. Kim SW, Choi HM (2014) Enhancement of thermal, mechanical and barrier properties of ethylene vinyl alcohol copolymer by incorporation of graphene nanosheets effect of functionalization of graphene oxide. *High Perform Polym* 27: 694-704
  23. Ahn TO, Kim CK, Kim BK, Jeong HM, Huh JD (1990) Binary blends of nylons with ethylene vinyl alcohol copolymers: Morphological, thermal, rheological and mechanical behavior. *Polym Eng Sci* 30: 341-349
  24. Yeh J-T, Huang S-S, Heng-Yi C (2005) White spirit permeation resistance of polyethylene, polyethylene/modified polyamide, and polyethylene/blends of modified polyamide and ethylene vinyl alcohol bottles. *Polym Eng Sci* 45: 25-32
  25. Park SH, Lee GJ, Im SS, Suh KD (1998) Ethylene vinyl alcohol copolymer/high density polyethylene blends compatibilized through functionalization. *Polym Eng Sci* 38: 1420-1425
  26. Thomas S, Grohens Y, Jyotishkumar P (2014) Characterization of polymer blends: Miscibility, morphology and interfaces. John Wiley & Sons
  27. Thomas S, Shanks R, Chandrasekharakurup S (2013) Nanostructured polymer blends. Vol. 1. William Andrew
  28. Kamal M, Garmabi H, Hozhabr S, Arghyris L (1995) The development of laminar morphology during extrusion of polymer blends. *Polym Eng Sci* 35: 41-51
  29. Samios CK, Kalfoglou NK (1998) Compatibilization of poly (ethylene-co-vinyl alcohol)(EVOH) and EVOH/HDPE blends with ionomers. Structure and properties. *Polym* 39: 3863-3870
  30. Wang Q, Qi R, Shen Y, Liu Q, Zhou C (2007) Effect of high-density polyethylene-g-maleic anhydride on the morphology and properties of (high-density polyethylene)/(ethylene–vinyl alcohol) copolymer alloys. *J Appl Polym Sci* 106: 3220-3226
  31. Kalfoglou NK, Samios CK, Papadopoulou CP (1998) Compatibilization of poly (ethylene-co-vinyl alcohol)(EVOH) and EVOH–HDPE blends: Structure and properties. *J Appl Polym Sci* 68: 589-596
  32. Lee SY, Kim SC (1997) Laminar morphology development and oxygen permeability of LDPE/EVOH blends. *Polym Eng Sci* 37: 463-475
  33. Lee S-Y, Kim SC (1998) Effect of compatibilizer on the crystallization, rheological, and tensile properties of LDPE/EVOH blends. *J Appl Polym Sci* 68: 1245-1256
  34. Park SH, Lee GJ, Im SS, Do Suh K (1998) Ethylene vinyl alcohol copolymer/high density polyethylene blends compatibilized through functionalization. *Polym Eng Sci* 38: 1420-1425
  35. Okada A, Usuki A (2006) Twenty years of polymer-clay nanocomposites. *Macromol Mater Eng* 291: 1449-1476
  36. Tsai Y, Wu J-H, Leu M-T (2011) Influence of organoclay dispersed state of poly (ethylene glycol-co-1, 3/1, 4-cyclohexanedimethanol terephthalate)/organoclay nanocomposites on their characteristics. *Polym Adv Technol* 22: 2319–2324
  37. Landel RF, Nielsen LE (1993) Mechanical properties of polymers and composites. CRC Press
  38. Khosrokhavar R, Naderi G, Bakhshandeh GR, Ghoreishy MHR (2011) Effect of processing parameters on PP/EPDM/organoclay nanocomposites using Taguchi analysis method. *Iran Polym J* 20: 41-53
  39. Johnson MB, Wilkes GL (2001) Microporous membranes of polyoxymethylene from a melt-extrusion process:(I) effects of resin variables and extrusion conditions. *J Appl Polym Sci* 81: 2944-2963

40. Johnson MB, Wilkes GL (2002) Microporous membranes of polyoxymethylene from a melt-extrusion process:(II) Effects of thermal annealing and stretching on porosity. *J Appl Polym Sci* 84: 1762-1780
41. Yu T-H, Wilkes GL (1996) Orientation determination and morphological study of high density polyethylene (HDPE) extruded tubular films: Effect of processing variables and molecular weight distribution. *Polymer* 37: 4675-4687